On the Inclusion of Temperature in the Friction Model of Industrial Robots

Luca Simoni [*] **Manuel Beschi** [**] **Giovanni Legnani** [*] **Antonio Visioli** [*]

[*] *Dipartimento di Ingegneria Meccanica e Industriale,
University of Brescia, Brescia, Italy
(e-mail: {l.simoni002,giovanni.legnani,antonio.visioli}@unibs.it).*
[**] *Instituto di Tecnologie Industriali e Automazione, National Research
Council, Milan, Italy (e-mail: manuel.beschi@itia.cnr.it)*

Abstract: This paper deals with a modelling technique that takes into account the effects of the temperature in the joint friction of industrial robot manipulators. In particular, it is shown that a general friction model can be suitably modified by explicitly considering the temperature as a parameter. This allows to estimate the friction term accurately in different operating conditions without the direct measurement of the joint internal temperature, which makes the overall technique suitable to apply in practical cases. Experimental results show the effectiveness of the methodology.

Keywords: Industrial manipulators, joint friction, temperature effects, modelling, parameters estimation.

1. INTRODUCTION

The integration of mechanical and control designs is nowadays recognized to be a very important issue in robotics and, more in general, in mechatronics. In fact, in order to create machines that are able to achieve better and better precision, mechanical and control engineers need to take into account all the different phenomena that might arise and the effects they introduce in the performance. Example of these phemomena are friction, elasticities and vibrations. Indeed, friction is one of the most known undesired phenomenon. It appears when there is the relative motion of two surfaces that are in contact, or when a body moves inside a fluid. The main effects of friction are the heating of the surfaces in contact, the loss of energy and, sometimes, chattering during low speed motions. Friction depends on a large variety of phenomena such as temperature, humidity, type of surfaces material, the presence of lubricant and its type, the velocity of motion, and so on (Marton, 2011). In fact, having a complete model that is able to describe friction torque or force depending on all these factors is almost impossible. Nevertheless, many friction models have been proposed in the literature in order to represent friction torque in the most appropriate way (see, for example (Andersson et al., 2007)). In industrial robots, the knowledge of the joint friction torque or force can be usefully exploited to improve the performance in motion control tasks and also in other tasks such as force control or manual guidance.

Friction models are usually divided into two different types: static and dynamic models (Olsson et al., 1998). The static models are the ones in which the relation between friction force or torque and the independent variable (usually speed) is fixed. Examples of friction static models are the Coulomb model, in which friction force is constant and it depends on the sign of the velocity, and the viscous model, in which friction force is linearly dependent on the velocity. Other static models are, for example, the Stribeck model, in which an exponential function represents the transition between static friction (friction force when the velocity is zero) and dynamic friction (friction force when the velocity is not zero) or the polynomial one (see (Visioli and Legnani, 2002; Simoni et al., 2015; Legnani et al., 2016)), in which a polynomial function describes the relation between speed of motion and friction force.

On the contrary, dynamic models are those in which friction force or torque is dependent on a state function that is able to consider also the history of the system, and not only the actual situation like the static models. Example of dynamic models are the Dahl model and its extended versions, the LuGre model and its extensions, the Leuven model or other more complex models like the Maxwell-slip one and its extensions and generalizations (van Geffen, 2009).

In order to compensate friction force, a lot of different techniques have been proposed in robotics (Bona and Indri, 2005). The most common technique consists in the application of a feedforward strategy. In order to take into account possible unmodelled parts in the friction model, the use of an adaptive strategy has also been suggested in the literature (Jatta et al., 2006). In other works the use of neural networks (Selmic and Lewis, 2002) or the use of observer based techniques (Mallon et al., 2006) has been proposed.

Recently, the role of the temperature in friction models has been highlighted, as it has been recognized that this is an important issue (Bittencourt and Axelsson, 2014). In particular, modelling strategies that do not require a measurement of the joint temperature have been pursued (Simoni et al., 2015; Carlson et al., 2016) as the use of additional sensors is somewhat impractical in an industrial framework.

In this paper we further develop the method already proposed in (Simoni et al., 2015) for a polynomial friction model, by extending it to a more complex friction model that takes into account the Stribeck effect explicitly (by means of an exponential term). In this way, we show that the idea of changing the model parameters linearly with the temperature can be applied in a more general framework, provided that suitable identification experiments are performed.

The main advantage of the use of the model proposed in this paper, with respect to, for example, an adaptive friction model, is related to possible contacts between the robot and the enviromnent. It is in fact clear that the adaptivity has to be stopped during the interaction time between the robot and the environment and, if the contact time interval is long, it can bring to friction estimation errors.

2. STRIBECK-POLYNOMIAL FRICTION MODEL

As already mentioned in the introduction, if the joint internal temperature does not change, the static relation between the joint velocity and the friction torque can be expressed in different forms. One of them is the polynomial form, which is usually able to model the friction term satisfactorily at both low and high velocities, including also the Stribeck effect (Simoni et al., 2015). However, in some cases (as it will be clear in section 3 where we will show the different temperature effects at low and high velocities), it might be useful to expand this relation by adding a term that is able to explicitly consider the Stribeck effect (see (van Geffen, 2009)) in order to better consider the variation during the passage between static and dynamic friction. In this way, the polynomial function can consider the (nonlinear) viscous friction behaviour while the Stribeck part is used to represent friction torque at low velocities.

The relation between friction torque and velocity can be therefore expressed as the sum between a polynomial term

$$\tau_{fpol} = \left[c_0 + c_1 \left| \omega \right| + c_2 \left| \omega \right|^2 + c_3 \left| \omega \right|^3 \right] \mathrm{sgn}(\omega) \qquad (1)$$

with a Stribeck term that can be effectively described using a simple exponential function:

$$\tau_{fstr} = c_4 e^{-h|\omega|} \mathrm{sgn}(\omega) \qquad (2)$$

that is,

$$\tau_f = \left[c_0 + c_1 \left| \omega \right| + c_2 \left| \omega \right|^2 + c_3 \left| \omega \right|^3 + c_4 e^{-h|\omega|} \right] \mathrm{sgn}(\omega) \qquad (3)$$

where ω is the joint speed of motion, c_0, c_1, c_2 and c_3 are the coefficients of the polynomial function τ_{fpol} and c_4 and h are the coefficients of the Stribeck function τ_{fstr}. It is important to notice that coefficient c_4 can be expressed as $c_4 = c_{str} - c_0$ as explained in (van Geffen, 2009).

A symmetric function that relates the friction torque with the velocity is considered. It means that friction torque has, in magnitude, the same values for positive and negative velocities.

By considering each joint of the robot separately from the others for the sake of simplicity (although the procedure can be easily generalized to consider all of them at the same time), the coefficients c_0, c_1, c_2, c_3 and c_4 are estimated by moving each joint of the robot from a point to another one with different velocities from 1% to 100% of the maximum one. The duration of the point-to-point motions has to be sufficient to allow the joint to reach the maximum speed. The parameter h is estimated before the others by using the *fmincon* Matlab function, and it is kept fixed. In order to compute the value of the cost function, that is, the sum of the square errors between the model values and the experimental ones, only an a posteriori analysis can demonstrate if the choice of h is appropriate. It can be done by comparing the estimated friction torque with the one obtained from the experimental data: roughly speaking, if the results are superimposed, the choice of h is correct, otherwise it is necessary to choose another value of h. In order to select a good value of the parameter h for the initial guess of the *fmincon* Matlab function, the following empirical rules can be useful:

- decide the percentage of maximum speed at which value the Stribeck effect can be considered negligible and denote it as $\tilde{\omega}$;
- considering that the negative exponential effect lose its influence after five times the time constant, the value of h has to be selected as $h = 5 \frac{1}{|\tilde{\omega}|}$

In this way, the exponential value becomes almost zero after five times the speed Stribeck constant. Considering this type of motion, that is a single joint one, it is possible to write the torque balance of the considered joint:

$$\tau = J\dot{\omega} - \tau_f - \tau_w \tag{4}$$

where J is the inertia of the joint, and τ_f and τ_w are the torques related to the friction and the weight of the link, respectively.

At this point it is possible to expand all the terms in (4), yielding

$$\begin{aligned}\tau = & J\dot{\omega} - c_0 \operatorname{sgn}(\omega) - c_1\omega - c_2\omega^2 \operatorname{sgn}(\omega) - c_3\omega^3 \\ & - c_4 e^{-h|\omega|} \operatorname{sgn}(\omega) - P_x \cos(\theta) + P_y \sin(\theta)\end{aligned} \tag{5}$$

where it is worth noting that the torque related to the link weight is

$$\tau_w = P_x \cos(\theta) - P_y \sin(\theta) \tag{6}$$

where θ is the measured joint position and

$$P_x = mgl \cos(\gamma) \quad P_y = mgl \sin(\gamma), \tag{7}$$

where g is the gravity acceleration, l is the distance between the axis of rotation of the considered joint and the centre of mass of the link, m is the mass of the link, and γ is the angle between θ and the centre of mass of the link.

Now, considering all the n sampled data of the trial, it is possible to express (5) in matrix form as

$$\bar{\tau} = \mathbf{M}\mathbf{X} \tag{8}$$

where the measured motor torque vector is

$$\bar{\tau} = \begin{bmatrix} \tau_1 & \tau_2 & \dots & \tau_n \end{bmatrix}^T \tag{9}$$

the measured matrix data is

$$\mathbf{M} = \begin{bmatrix} \dot{\omega}_1 & -\operatorname{sgn}(\omega_1) & -\omega_1 & -\omega_1^2 \operatorname{sgn}(\omega_1) & -\omega_1^3 & -e^{-h|\omega_1|} \operatorname{sgn}(\omega_1) & -\cos(\theta_1) & \sin(\theta_1) \\ \dot{\omega}_2 & -\operatorname{sgn}(\omega_2) & -\omega_2 & -\omega_2^2 \operatorname{sgn}(\omega_2) & -\omega_2^3 & -e^{-h|\omega_2|} \operatorname{sgn}(\omega_2) & -\cos(\theta_2) & \sin(\theta_2) \\ \vdots & \vdots & \vdots & \vdots & \vdots & \vdots & \vdots & \vdots \\ \dot{\omega}_n & -\operatorname{sgn}(\omega_n) & -\omega_n & -\omega_n^2 \operatorname{sgn}(\omega_n) & -\omega_n^3 & -e^{-h|\omega_n|} \operatorname{sgn}(\omega_n) & -\cos(\theta_n) & \sin(\theta_n) \end{bmatrix} \tag{10}$$

and the vector of coefficients to estimate is

$$\mathbf{X} = \begin{bmatrix} J & c_0 & c_1 & c_2 & c_3 & c_4 & P_x & P_y \end{bmatrix}^T. \tag{11}$$

The coefficients can be estimated using the standard least square method expressed as

$$\mathbf{X} = \mathbf{M}^+ \bar{\tau} \tag{12}$$

where $\mathbf{M}^+$ represents the Moore-Penrose pseudo-inverse of the matrix $\mathbf{M}$.

3. MODELING TEMPERATURE EFFECT

One of the most important characteristics of friction is that, as explained for example in (Simoni et al., 2015; Kozlowski, 1998; Carlson et al., 2016), it changes during robot operations. In particular, in (Simoni et al., 2015; Legnani et al., 2016) it has been shown that, for the robot considered therein, the friction torque value decreases for all the velocities if the joint internal temperature increases and vice versa. However, for the robot considered in this paper, the temperature effect has been found to be slightly different, as it can be seen in Fig. 1, where the friction functions obtained by considering experimental data collected each four minutes of continuous robot operations started after the robot has been at rest for a long period are plotted. It appears that, when the speed of motion is less than a small percentage of the maximum joint speed (about 5% or 10%), the Stribeck effect becomes significant and, most of all, the value of friction torque increases with temperature (see Fig. 2), while for higher speed friction

decreases with temperature. This behaviour can be explained by taking into account that the used lubricant is more effective if it has a high viscosity at low velocities (because in this case it is more capable to separate the two surfaces in contact by means of the generation of a fluid film) and a low viscosity at high velocities (because in this case the separation of the two surfaces is due mainly to the velocity and the lubricant reduces its opponent force). Thus, by taking into account that the lubricant viscosity decreases when the temperature increases, we have that if the relative speed between the surfaces in contact is high, when the temperature increases the lubricant becomes less viscous and the friction force decreases. However, when the relative speed between the surfaces in contact is low, the less viscous lubricant has more difficulties to create a film between the surfaces and therefore, in this case, the friction force increases (Pirro et al., 2016).

In order to compensate for friction torque during joint motion, these effects have to be suitably taken into account, as it is done in this paper. For this purpose, model (3) has to be suitably adjusted. The new model comes from the thermal power balance of the joint

$$W_{acc} = W_{in} - W_{out} \tag{13}$$

where

$$W_{in} = \tau_f \omega \tag{14}$$

is the injected thermal power in the joint, which depends directly on friction torque τ_f and on the speed of motion ω,

$$W_{out} = K(T - T_{env}) \tag{15}$$

is the dissipated thermal power, which is related to the difference between the actual joint internal temperature T and the environmental one T_{env} multiplied by the thermal exchange coefficient K, and

$$W_{acc} = C\frac{dT}{dt} \tag{16}$$

is the thermal power that is accumulated inside the robot joint, which is proportional to the thermal capacity C. The temperature effect can be modelled by changing the polynomial parameters linearly with the temperature as

$$c_i = c_{i,0}\left[\alpha_1\left(T - T_0\right) + \beta_1\right] \quad \text{for} \quad i = 0, \dots, 3 \tag{17}$$

where α_1 and β_1 are coefficients that express the linearity between the polynomial coefficients and the joint internal temperature, and $c_{i,0}$, $i = 0, \dots, 3$ are the coefficients values for a certain joint internal temperature T_0. In order to include the Stribeck effect in this model, a similar linear relation must be assumed. Considering that the polynomial linear parameters α_1 and β_1 can be different with respect to the Stribeck ones due to the fact that the Stribeck effect has a different behaviour with respect to the polynomial curve (see Fig. 2), the linear relation for the Stribeck coefficient becomes

$$c_4 = c_{4,0}\left[\alpha_2\left(T - T_0\right) + \beta_2\right] \tag{18}$$

where α_2 and β_2 are coefficients that express the linearity between the Stribeck coefficient and the joint internal temperature, and $c_{4,0}$ is the Stribeck coefficient value for a certain joint internal temperature T_0. Thus, the joint temperature variation considering the Stribeck term can be expressed as
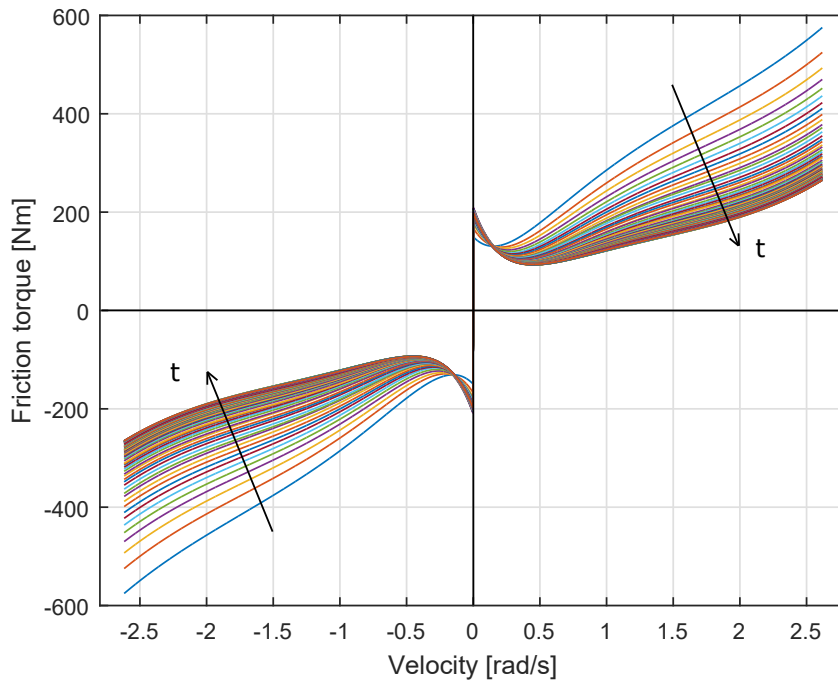

Fig. 1. Modification of the friction torque curve during continuous robot operations (intervals of four minutes) started after the robot has been at rest for a long time.
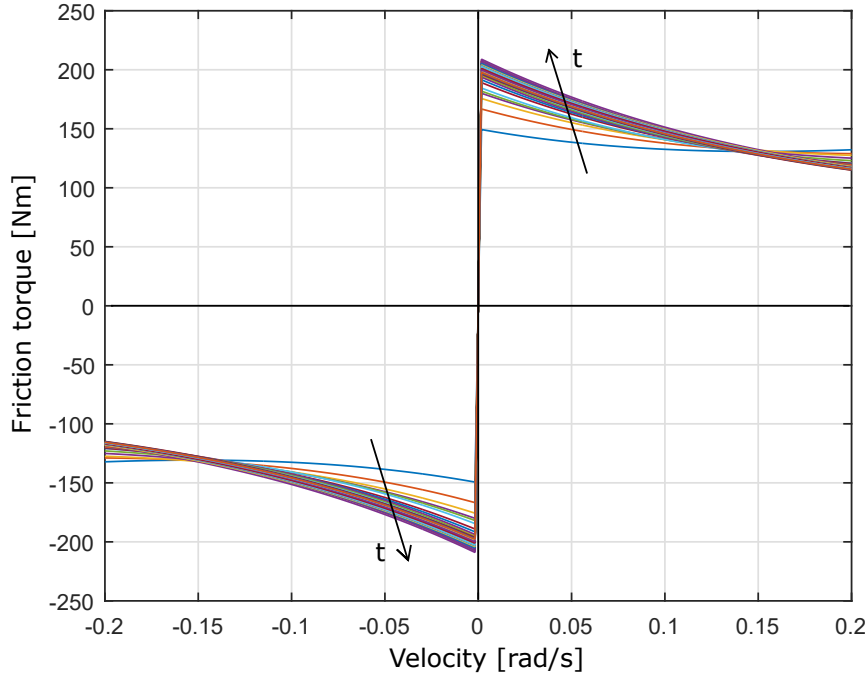
Fig. 2. Zoom of Fig. 1 for low velocities.

$$
\begin{cases}
\dfrac{dT}{dt} = \left[\tau_f(T)\omega - K(T - T_{env}) \right] \dfrac{1}{C} & (19) \\[2mm]
\tau_f(T) = \tau_{f0pol} \left[\alpha_1(T - T_0) + \beta_1 \right] \\
\qquad\quad + \tau_{f0str} \left[\alpha_2(T - T_0) + \beta_2 \right] & (20)
\end{cases}
$$

where (20) can be also written as

$$
\tau_f(T) = \tau_{fpol}(T) + \tau_{fstr}(T) \tag{21}
$$

in which $\tau_{fpol}(T)$ is the polynomial part of the friction torque at temperature T

$$
\tau_{fpol}(T) = \left(c_0 + c_1 |\omega| + c_2 |\omega|^2 + c_3 |\omega|^3 \right) \mathrm{sgn}(\omega) \tag{22}
$$

and $\tau_{fstr}(T)$ represents the exponential Stribeck term at temperature T

$$
\tau_{fstr}(T) = c_4 e^{-h|\omega|} \,\mathrm{sgn}(\omega). \tag{23}
$$

It is worth stressing that in (22) and (23) the friction parameters $c_{i,0}$, with $i = 0, \ldots, 4$, are updated using (17) and (18).

Parameters α_1, β_1, α_2, β_2, K, C must be estimated after having determined the polynomial parameters (c_0, c_1, c_2, c_3) and the Stribeck ones (c_4, h). Further details are explained in section 4.

At this point it is worth highlighting that, during the parameters identification procedure, values of β_1 and β_2 different from 1 are expected as these values may be actually obtained only in case of perfect modelling. Furthermore, a negative and much smaller than one value of parameter α_1, and a positive and much smaller than one value of parameter α_2 are expected.

The solution of the differential equation (19), by considering $T(0) = T_0$ as initial condition, results

$$
\begin{aligned}
T(t) = & \frac{\beta_1 \omega \tau_{f0pol} + \beta_2 \omega \tau_{f0str} + K T_{env}}{K + \alpha_2 \omega \tau_{f0str} - \alpha_1 \omega \tau_{f0pol}} \\
& + \frac{\alpha_2 T_0 \omega \tau_{f0str} - \alpha_1 T_0 \omega \tau_{f0pol}}{K + \alpha_2 \omega \tau_{f0str} - \alpha_1 \omega \tau_{f0pol}} \\
& + \gamma e^{\frac{+\alpha_1 \omega \tau_{f0pol} - \alpha_2 \omega \tau_{f0str} - K}{C} t}
\end{aligned} \tag{24}
$$

where

$$
\begin{aligned}
\gamma = & \frac{K T_0 + \alpha_2 T_0 \omega \tau_{f0str} - \alpha_1 T_0 \omega \tau_{f0pol} - K T_{env}}{K + \alpha_2 \omega \tau_{f0str} - \alpha_1 \omega \tau_{f0pol}} \\
& + \frac{-\beta_1 \omega \tau_{f0pol} - \beta_2 \omega \tau_{f0str}}{K + \alpha_2 \omega \tau_{f0str} - \alpha_1 \omega \tau_{f0pol}} \\
& + \frac{-\alpha_2 T_0 \omega \tau_{f0str} + \alpha_1 T_0 \omega \tau_{f0pol}}{K + \alpha_2 \omega \tau_{f0str} - \alpha_1 \omega \tau_{f0pol}}.
\end{aligned} \tag{25}
$$

The resulting time constant of the first-order system is

$$t_c = -\frac{C}{+\alpha_1 \omega \tau_{f0pol} - \alpha_2 \omega \tau_{f0str} - K} \tag{26}$$

and this can be used to determine the duration of the time intervals after which the value of the joint temperature has to be updated. In fact, from a practical point of view, the value of the estimated temperature should not be updated at each sampling period but, on the contrary, it should be updated after time intervals of a selected duration (for example, after each cycle if the robot performs a repetitive task). These time intervals have to be in any case significantly smaller than this time constant and therefore a good choice for their selection is one order of magnitude, that is, $t_c/10$.

In this context, it is necessary to modify (19)-(20)as follows:

$$\begin{cases} \dfrac{\Delta T}{\Delta t} = \left[\tau_{f,RMS} \bar{\omega} - K(T - T_{env}) \right] \dfrac{1}{C} & (27) \\[2mm] \tau_{f,RMS} = \tau_{f0pol,RMS} \left[\alpha_1 (T - T_0) + \beta_1 \right] \\ \qquad\quad + \tau_{f0str,RMS} \left[\alpha_2 (T - T_0) + \beta_2 \right] & (28) \end{cases}$$

where $\tau_{f0pol,RMS}$ is the RMS value of the polynomial part of the friction torque and $\tau_{f0str,RMS}$ is the RMS value of the Stribeck one, both calculated in the given time interval. Note that $\tau_{f0pol,RMS}$ and $\tau_{f0str,RMS}$ are obtained by considering the first time interval of motion after the robot has been at rest for a long period, so that it is possible to consider $T = T_0 = T_{env}$. Then, $\tau_{f,RMS}$ represents the RMS friction torque value related to a certain time interval, and

$$\bar{\omega} = \frac{\text{mean}(\tau_f \omega)}{\tau_{f,RMS}} \tag{29}$$

can be considered an equivalent thermal velocity and represents the speed value that permits to obtain the mean friction power during a given interval, considering as friction torque the RMS one.

Summarizing, in order to apply the model, the following steps has to be followed:

- at the beginning of the robot operations, if the robot has been at rest for a long time (some hours), the computation of friction torque τ_f is simply given by (21) with joint internal temperature $T = T_{env}$;
- at the end of the first time interval, the value of $\tau_{f0,RMS}$ is computed as the sum of the polynomial and Stribeck contributions;
- using (29) the value of $\bar{\omega}$ is computed;
- the change of the temperature is computed by using (27);
- the following passages can then be repeated at each time interval in order to find the value of the joint internal temperature T:
    - application of (28) (by using the temperature value of the previous step) in order to find $\tau_{f,RMS}$;
    - application of (27) to find the joint internal temperature modification;
    - estimation of the friction torque using (21) with the updated value of temperature T.

4. IDENTIFICATION EXPERIMENTS

Experiments have been performed with the Comau SMART NS16 manipulator described in (Simoni et al., 2015).

The devised model only requires the environmental temperature to be measured. In order to estimate the other parameters, it is necessary to perform suitable experiments.

The coefficients $c_{i,0}$ with $i = 1 \ldots 4$ and k of the friction functions (see (3), (17) and (18)) are obtained by applying the method explained in section 2 to the first cycle of the trials. In fact, the first cycle is performed after a robot rest of about 10 hours, thus, it is possible to consider the joint temperature value equal to the environmental one ($T_0 = T_{env}$).

A possible choice for the estimation of the other parameters α_1, β_1, α_2, β_2, K and C can be to apply a similar procedure to the one described in (Simoni et al., 2015). However, the trajectory to be followed has to be slightly modified in order to better estimate both the inertia seen by the joint and the Stribeck effect.

In order to estimate accurately the thermal model parameters, it is necessary to apply different thermal powers to the joints. The identification can be therefore done by performing four different types of trials for each joint, where the robot is operated after a long time of rest (about 10 hours in order to consider $T = T_0 = T_{env}$). Each trial is composed by 100 cycles and each cycle is composed by four time intervals of one minute each one. A different duty cycle (DC) of motion (from 25% to 100%) is associated to each trial. In particular, (see Fig. 3):

- for $DC = 25\%$, the joint moves only for the first time interval (t1) and it is at rest for the other three ones (t2, t3 and t4);
- for $DC = 50\%$, the joint moves only for the first two time intervals (t1 and t2) and it is at rest for the other two (t3 and t4);
- for $DC = 75\%$, the joint moves during the first three time intervals (t1, t2 and t3) and it is at rest for the last one (t4);
- for $DC = 100\%$, the joint moves during all the time intervals (t1, t2, t3 and t4).

The performed trajectory is a single joint motion from two different points, spanning the velocities between 1% and 100% of the maximum joint speed in each cycle. It appears that a different thermal power injected in the joint is associated to each duty cycle of motion, therefore, the internal temperature reached by the joint is different in the four cases (see Fig. 4). The parameters are then estimated by considering all the data collected in the four trials and by minimizing the sum of the square errors between the estimated friction torque and the one obtained from the experimental data.

In this section, only results of the second joint of the robot are reported for the sake of brevity, however, the other joints behaves in a similar way. The values of the estimated parameters for joint 2 are shown in Table 1.
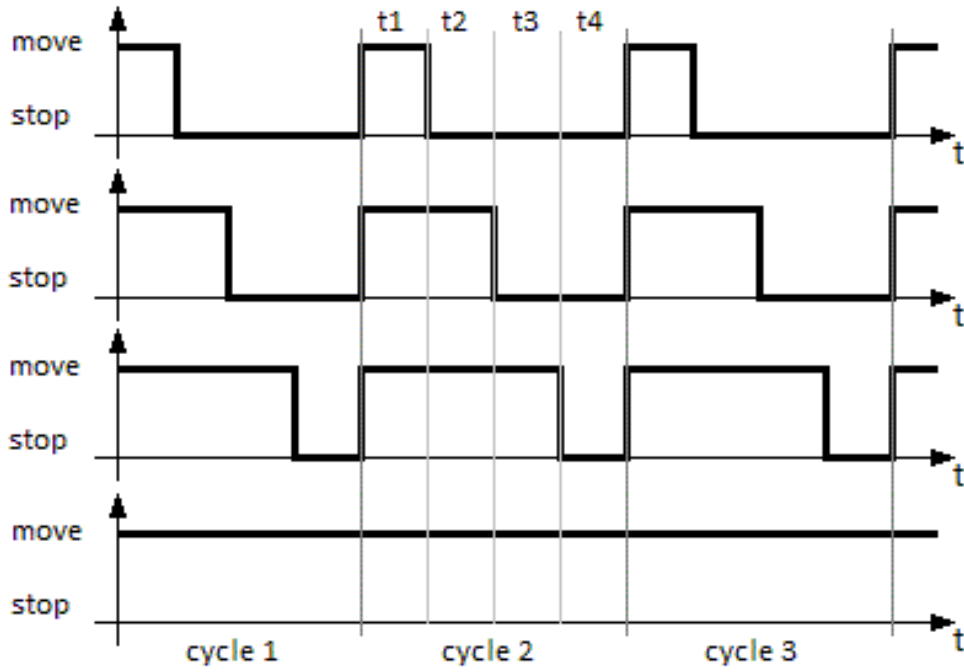
Fig. 3. The different robot cycles used in the identification trials ($DC = 25\%, 50\%, 75\%, 100\%$).
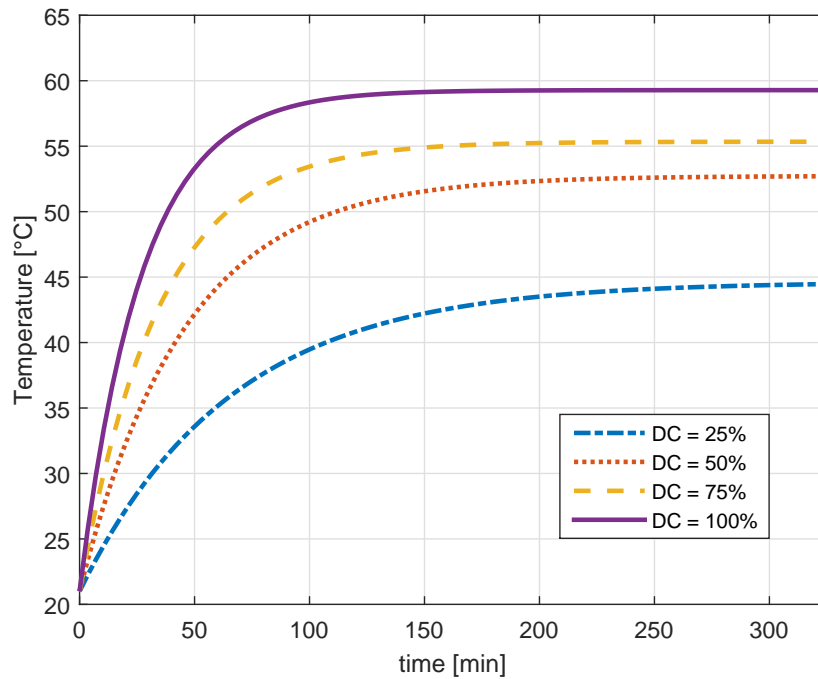

Fig. 4. Estimated joint internal temperature for the four different duty cycles of motion used in the identification trials.

Table 1. Estimated model parameters for joint 2.

Estimated parameter	Value
α_1	-0.013793
β_1	0.938016
α_2	0.027611
β_2	0.516596
K	2.033073
C	13553.36

The results of friction torque-velocity curve during working time, that is, for different joint internal temperatures, for the $DC = 100\%$ trial are shown in Fig. 5. The values of the heating time constants for joint 2 are shown in Table 2.
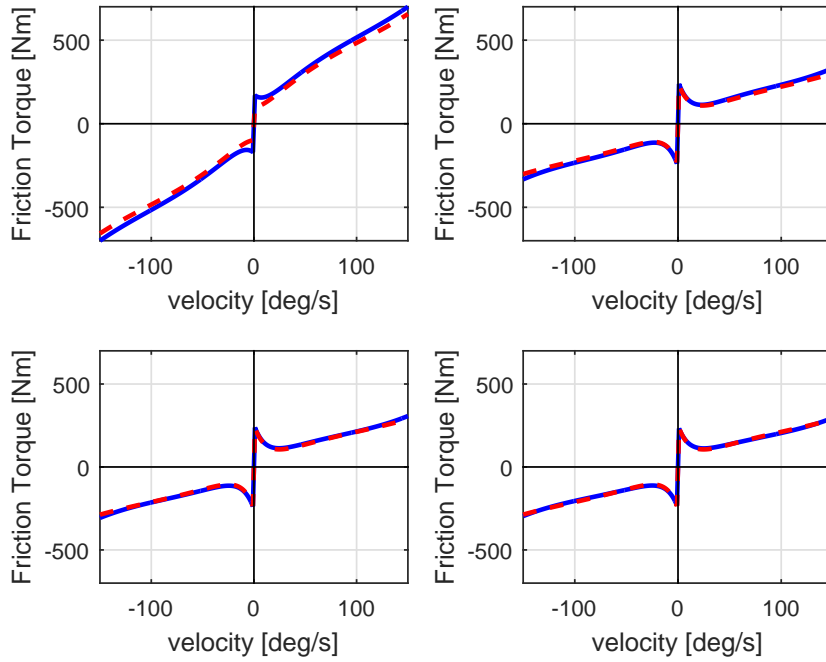
Fig. 5. Model identification, duty cycle $DC = 100\%$. Torque versus velocity plot. Friction torque obtained with experimental data (blue solid line) and identified with the proposed model (red dashed line). Top left: results after 4 minutes. Top right: after 104 minutes. Bottom left: after 204 minutes. Bottom right: after 304 minutes.

Table 2. Estimated time constants for joint 2 for different duty cycles.

Duty cycle [%]	Time constant [min]
25	65.73
50	45.46
75	34.53
100	26.94

5. VALIDATION EXPERIMENTS

After having estimated the values of α_1, β_1, α_2, β_2, K and C, that is, after having calibrated the model, validation experiments have been performed for each joint. In order to do that, single joint motions are performed as explained in (Simoni et al., 2015). In particular,

- the duration of each cycle time is three minutes;
- the duty cycle of each trial is 100%;
- the trajectory repeated during each trial consists of following a velocity profile from 1% to 100% of the maximum velocity, increasing and decreasing the speed several times.

It is worth stressing that these trajectories are different from those applied in the identification phase.
Again only results related to joint 2 of the manipulator are shown for the sake of brevity. In Fig. 6 the comparison between the friction torque-velocity curve obtained from the experimental data and the one predicted by the proposed model (each 25 cycles, that is, after different time intervals) is shown.
In Fig. 7 the friction torque obtained with experimental data during different motion intervals is shown together with that estimated by model. It appears that the estimation accuracy of the model is kept at a satisfactory level in spite of the friction changes along the time because of the temperature. Indeed, it appears that the model is capable to describe effectively the temperature effects both at low and high velocities.
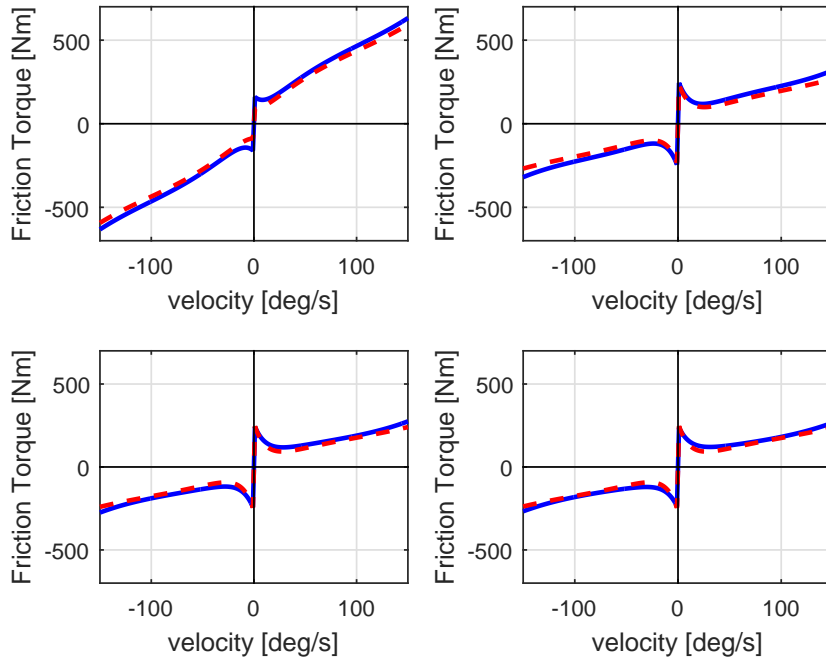
Fig. 6. Model validation. Torque versus velocity plot. Friction torque obtained with experimental data (blue solid line) and estimated with the proposed model (red dashed line). Top left: after 3 minutes. Top right: after 78 minutes. Bottom left: after 153 minutes. Bottom right: after 228 minutes.
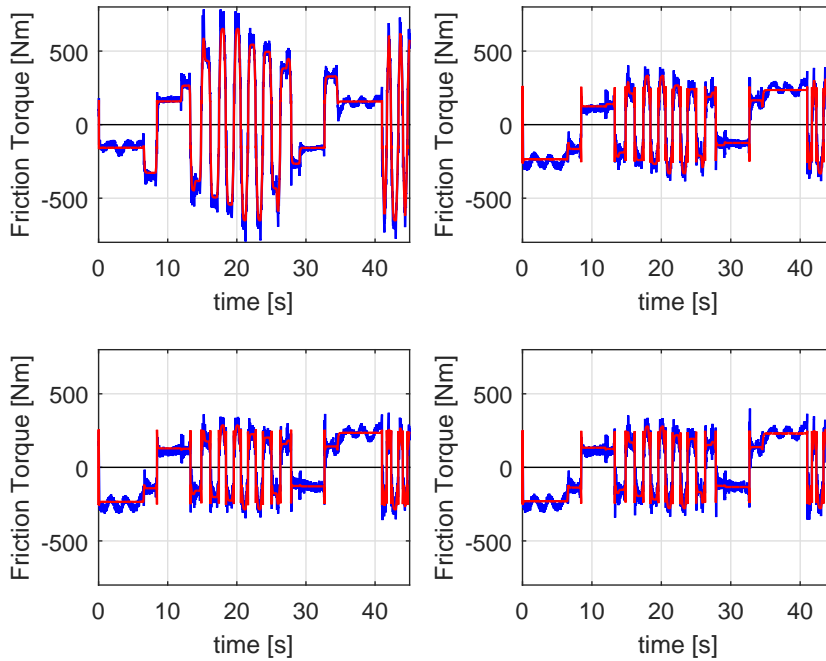

Fig. 7. Model validation. Friction torque obtained with experimental data (blue solid line) and estimated with the proposed model (red dashed line) during a motion interval. Top left: after 3 minutes. Top right: after 78 minutes. Bottom left: after 153 minutes. Bottom right: after 228 minutes.

6. CONCLUSIONS

In this work it has been shown that the method described in (Simoni et al., 2015) and analysed in (Legnani et al., 2016) to model the effects of temperature for a particular (polynomial) joint friction model can be extended to a more general model where the Stribeck phenomenon (described by an exponential term) is taken into account explicitly. The proposed extension maintains the

same characteristics of the base model, that is, the model parameters change linearly with the temperature, but permits to describe different temperatures related behaviours for the friction at low and high velocities. Further, it is not necessary to measure the joint internal temperature, but just an estimation is sufficient to take into account friction torque variation during robot operations. In this way, only the measure of the environmental temperature is needed to use the model once it has been identified and this makes the method suitable to apply in the industrial context.

ACKNOWLEDGEMENTS

REFERENCES

Andersson, S., Söderberg, A., and Björklund, S. (2007). Friction models for sliding dry, boundary and mixed lubricated contacts. *Tribology International*, 40(4), 580–587.

Bittencourt, A.C. and Axelsson, P. (2014). Modeling and experiment design for identification of wear in a robot joint under load and temperature uncertainties based on friction data. *IEEE/ASME Transactions on Mechatronics*, 19(5), 1694–1706.

Bona, B. and Indri, M. (2005). Friction compensation in robotics: an overview. In *Proceedings of the 44th IEEE Conference on Decision and Control and the European Control Conference*, 4360–4367. Seville (E).

Carlson, F.B., Robertsson, A., and Johansson, R. (2016). Modeling and identification of position and temperature dependent friction phenomena without temperature sensing. In *Proceedings of the IEEE/RSJ International Conference on Intelligent Robots and Systems*, 3045–3051. Hamburg (D).

Jatta, F., Legnani, G., and Visioli, A. (2006). Friction compensation in hybrid force/velocity control of industrial manipulators. *IEEE Transactions on Industrial Electronics*, 53(2), 604–613.

Kozlowski, K.R. (1998). *Modelling and Identification in Robotics*. Springer-Verlag, London (UK).

Legnani, G., Simoni, L., Beschi, M., and Visioli, A. (2016). A new friction model for mechanical transmissions considering joint temperature. In *Proceedings of the ASME 2016 International Design Engineering Technical Conferences and Computers and Information in Engineering Conference*, V006T09A020–V006T09A020. Charlotte (US).

Mallon, N., van de Wouw, N., Putra, D., and Nijmeijer, H. (2006). Friction compensation in a controlled one-link robot using a reduced-order observer. *IEEE Transactions on Control Systems Technology*, 14(2), 374–383.

Marton, L. (2011). On-line lubricant health monitoring in robot actuators. In *Proceedings of the Australian Control Conference (AUCC)*, 167–172. Melbourne (Australia).

Olsson, H., Åström, K.J., de Wit, C.C., Gäfvert, M., and Lischinsky, P. (1998). Friction models and friction compensation. *European Journal of Control*, 4, 176–195.

Pirro, D.M., Webster, M., and Daschner, E. (2016). *Lubrication Fundamentals- Third Edition*. CRC Press, Boca Raton (USA).

Selmic, R.R. and Lewis, F.L. (2002). Neural-network approximation of piecewise continuous functions: Application to friction compensation. *IEEE Transactions on Neural Networks*, 13(3), 745–751.

Simoni, L., Beschi, M., Legnani, G., and Visioli, A. (2015). Friction modeling with temperature effects for industrial robot manipulators. In *Proceedings of the IEEE/RSJ International Conference on Intelligent Robots and Systems*, 3524–3529. Hamburg (D).

van Geffen, V. (2009). A study of friction models and friction compensation. Technical Report DCT 2009.118, Technische Universiteit Eindhoven, Department Mechanical Engineering, Dynamics and Control Technology Group, Eindhoven (NL).

Visioli, A. and Legnani, G. (2002). On the trajectory tracking control of industrial SCARA robot manipulators. *IEEE Transactions on Industrial Electronics*, 49(1), 224–232.